



# INSIGHTS INTO THE MAGNETIC ORIGIN OF $\text{Cu}_n\text{Cr}$ ( $n = 9 \div 11$ ) CLUSTERS: A SUPERPOSITION OF MAGNETIC AND ELECTRONIC SHELLS

Nguyen Thi Mai<sup>1,2</sup>, Ngo Thi Lan<sup>1,2,3</sup>, Nguyen Thanh Tung<sup>1,2,\*</sup>

<sup>1</sup>Graduate University of Science and Technology, VAST, 18 Hoang Quoc Viet, Ha Noi, Vietnam

<sup>2</sup>Institute of Materials Science, VAST, 18 Hoang Quoc Viet, Ha Noi, Vietnam

<sup>3</sup>University of Science, Thai Nguyen University, Tan Thinh, Thai Nguyen City, Thai Nguyen, Vietnam

\*Email: [tungnt@ims.vast.ac.vn](mailto:tungnt@ims.vast.ac.vn)

Received: 6 August 2019; Accepted for publication : 22 October 2019

**Abstract.** Interests in Cu-Cr sub-nanometer systems have been increasing due to the recently-found icosahedral  $\text{Cu}_{12}\text{Cr}$  cluster as a superatomic molecule, where the 3d-Cr and 4s-Cu electrons can phenomenologically form the 18-e molecular shell ( $1S^21P^61D^{10}$ ) of  $\text{Cu}_{12}\text{Cr}$ . In this report, we set out to investigate the energetically-preferred geometries and stabilities of  $\text{Cu}_n\text{Cr}$  ( $n = 9 \div 11$ ) clusters using the density-functional-theory calculations. It is found that not all of 3d-Cr electrons involve in the formation of the cluster shell and the remaining localized ones cause the magnetic moment of the clusters, which is different from what was believed. The calculated molecular diagram, natural orbital analysis, and spin-density computation are performed to elaborate our idea.

**Keywords:** Copper-chromium clusters, magnetic moment, superatoms, s-d hybridization.

**Classification number:** 2.2.1, 2.4.1, 4.10.4.

## 1. INTRODUCTION

In the field of advanced materials science, artificial atomic assemblies with structure sizes below nanometers have recently been of a great interest due to their potential as building blocks for novel nanostructured materials [1-10]. The most fascinating feature of atomic clusters is the anomalous change of their geometric and electronic structures upon adding or removing only a single atom [11]. This interesting property is exploited to create sustainable superatoms with desired functionalities that can replace or outperform existing elements in the Periodic table. In this regard, doping of copper clusters with different atoms is expected to tailor the structural, electronic, catalytic, and magnetic properties for applications in materials science, solid states chemistry, microelectronics and nanotechnology [6-10, 12-20]. For instance, the electronic structure of scandium-doped copper cluster cations  $\text{Cu}_n\text{Sc}^+$  were investigated. The  $\text{Cu}_{17}\text{Sc}$  cluster was found to be a superatomic molecule,  $\text{Cu}_{15}\text{Sc}$  was found to be a stable cluster with a large

dissociation energy and a closed electronic structure, hence this can be regarded as a superatom [21]. The nucleation energy and reactivity descriptors of  $\text{Cu}_n\text{M}$  ( $\text{M}=\text{Ni}, \text{Pd}, \text{Pt}; n = 1-4$ ) bimetallic nanoparticles supported on MgO (111) surface have been studied by density functional theory method and compared to their gas phase counterparts [15]. The magnetic properties of small  $\text{Cu}_n\text{TM}$  clusters ( $n = 3-7, 12; \text{TM}=\text{Ru}, \text{Rh}, \text{Pd}$ ) have been studied. The magnetic of  $\text{Cu}_n\text{TM}$  clusters are mainly affected by symmetry, coordination number and atomic distance [22]. The geometrical, electronic and magnetic properties of small  $\text{Cu}_n\text{Fe}$  ( $n = 1-12$ ) clusters have been investigated by using density functional. The  $\text{Cu}_7\text{Fe}$  cluster with a large energy gap (2.61 eV) can be perceived as a superatom [13].

Recently, the investigation on  $\text{Cu}_n\text{Cr}$  clusters ( $n = 9-16$ ) has found that  $\text{Cu}_{12}\text{Cr}$  is exceptionally stable and chemically inert as a superatomic molecule [23]. The magnetic moment of  $\text{Cu}_n\text{Cr}$  clusters is governed mainly by the interaction between  $d$ - $s$  valence orbitals of Cr and Cu atoms [23]. The magnetic moment of  $\text{Cu}_n\text{Cr}$  ( $n = 9-11$ ) clusters can be understood by incompleting electronic shell configuration  $1\text{S}^21\text{P}^61\text{D}^9$  for  $\text{Cu}_{11}\text{Cr}$ ,  $1\text{S}^21\text{P}^61\text{D}^8$  for  $\text{Cu}_{10}\text{Cr}$ , and  $1\text{S}^21\text{P}^61\text{D}^7$  for  $\text{Cu}_9\text{Cr}$ . In this report, we perform a quantitative analysis on the molecular diagram and cluster-spin density in order to provide a deeper understanding on the magnetism origin of  $\text{Cu}_n\text{Cr}$  ( $n = 9-11$ ) clusters.

## 2. COMPUTATIONAL METHOD

In order to study the  $\text{Cu}_n\text{Cr}$  clusters ( $n = 9-11$ ) we use the method of density functional theory (DFT) which is implemented in the Gaussian 09 software [24, 25]. We have recalculated the optimized geometries of  $\text{Cu}_n\text{Cr}$  clusters ( $n = 9-11$ ) using the BP86 functional with the basis sets cc-pvTZ-pp for Cu atom and cc-pvTZ for Cr atom to confirm the results presented in Ref. [23]. The previous investigation on  $\text{ScCu}_n$  clusters also indicated that results obtained by the BP86 functional are well-matched to experimental values [21]. The calculations are followed by frequency calculations to confirm the stationary structures are minimal. The electronic structure of  $\text{Cu}_n\text{Cr}$  global minima clusters were explored using the spin multiplicities, spin-density, the molecular orbital diagram and the natural orbital analysis of  $\text{Cu}_n\text{Cr}$  clusters.

## 3. RESULTS AND DISCUSSION

### 3.1. Optimized structures and spin multiplicities

The most stable optimized structures of the  $\text{Cu}_n\text{Cr}$  clusters with  $n = 9-11$  are illustrated in Figure 1. Firstly, the Gaussview program has been used to construct all possible structures of pure  $\text{Cu}_n$  clusters. Then a Cr atom has been added into the stable structures of the  $\text{Cu}_n$  clusters at different positions forming the  $\text{Cu}_n\text{Cr}$  clusters which are the input structures for the next optimization calculations. In the following, we denote each structure as n.x, in which n stands for number of Cu atoms in cluster  $\text{Cu}_n\text{Cr}$  and x is labeled as A, B, C and D for isomers with increasing order of energy.

**$\text{Cu}_9\text{Cr}$ .** A lot of isomers have been found, including some low-energy isomers. In the first isomer quartet 9.A, the Cr atom is encapsulated by a pentagonal pyramid and three Cu atoms. This is the most stable isomer of  $\text{Cu}_9\text{Cr}$  cluster. The quartet 9.B, doublet 9.C, and sextet 9.D have a slightly distorted form of 9.A with 0.43, 0.61 and 0.83 eV less stable than the ground state, respectively.

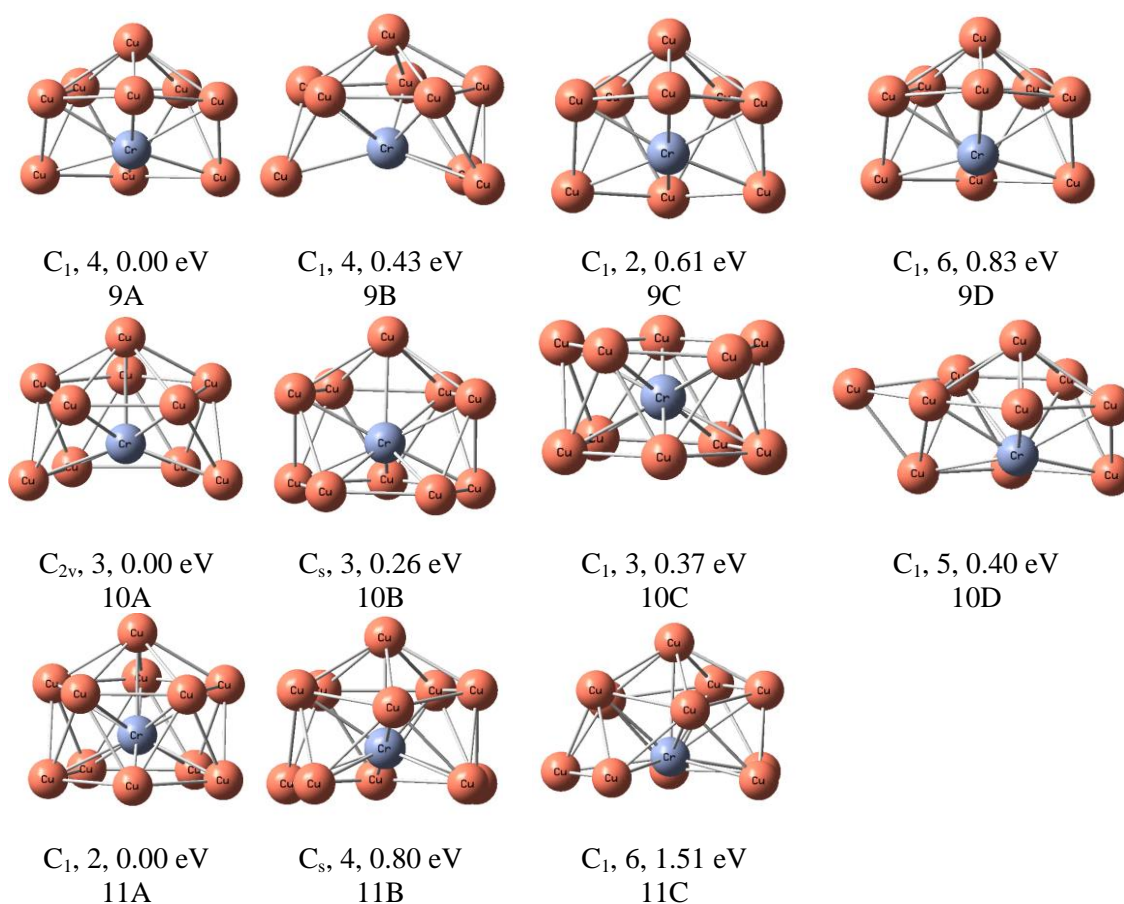


Figure 1. The ground-state structures of  $\text{Cu}_n\text{Cr}$  ( $n = 9-11$ ) clusters, and low-lying isomers for  $\text{Cu}_n\text{Cr}$  clusters. The point group, spin multiplicity, and energy difference compared to each ground state structure are given. The orange and violet balls represent Cu and Cr atoms, respectively.

**$\text{Cu}_{10}\text{Cr}$ .** The triplet 10.A, the Cr atom is surrounded by a pentagonal pyramid and an opened four-member  $\text{Cu}_4$  string. With a relative energy of 0.26 eV, the next isomer 10.B is composed of a Cr atom encapsulated by a square pyramid and a five-member  $\text{Cu}_5$  ring. The isomer 10.C has an anti-prism form, located at 0.37 eV above the 10.A. Other low-lying energy isomers, the quintet 10.D is unstable with 0.40 eV above the ground state 10.A.

**$\text{Cu}_{11}\text{Cr}$ .** The isomer 11.A in which the Cr atom captured by a pentagonal pyramid and a  $\text{Cu}_5$  five-member ring is the most stable isomer of  $\text{Cu}_{11}\text{Cr}$  cluster. Two next isomers 11.B and 11.C, having quartet and sextet states with a small distortion in geometry, are highly unstable.

The cluster magnetic states are very stable. For  $\text{Cu}_9\text{Cr}$ , the minimum energy required to switch the spin state (from quartet to doublet) is 0.61 eV. This value is 0.40 eV for  $\text{Cu}_{10}\text{Cr}$  (from triplet to quintet) and 0.80 eV for  $\text{Cu}_{11}\text{Cr}$  (from doublet to quartet) correspondingly.

### 3.2. Electronic and magnetic properties

In the previous work, the spin states of  $\text{Cu}_n\text{Cr}$  ( $n = 9-11$ ) clusters have been well explained by the phenomenological shell [23] in which six outermost valence electrons of Cr atom ( $3d^5 4s^1$ ) and  $n$   $4s^1$  valence electrons of Cu atoms are assumed to freely delocalize and jointly form a

molecular shell of the cluster. Taking that picture in mind, the quartet state of  $\text{Cu}_9\text{Cr}$  can be understood in accordance to the particular electronic shell of  $1S^21P^61D^7$  with three unpaired electrons. Similar to the cases of  $\text{Cu}_{11}\text{Cr}$  and  $\text{Cu}_{10}\text{Cr}$ , their electronic shell configuration are  $1S^21P^61D^9$  and  $1S^21P^61D^8$ , respectively. In order to quantitatively determine the origin of unquenched magnetic states, we perform the molecular diagram, local magnetic moments (LMM in  $\mu_B$ ), electron configurations of Cr atom and density of state analysis for  $\text{Cu}_n\text{Cr}$  ( $n = 9-11$ ) clusters. The results are shown in Fig. 2 and Table 1.

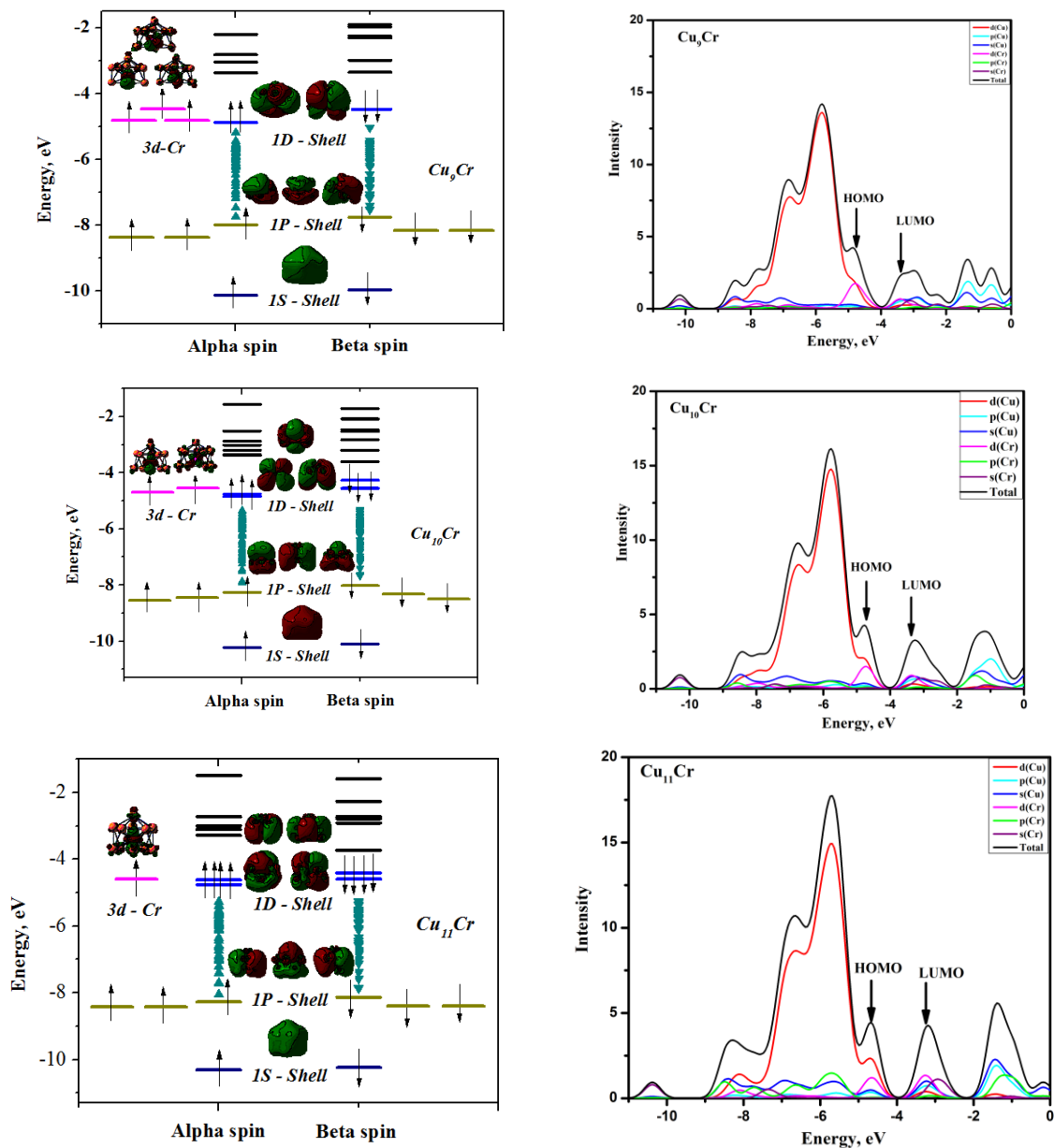


Figure 2. Total/partial DOS (right) and the molecular diagrams (left) of  $\text{Cu}_n\text{Cr}$  ( $n = 9-11$ ) clusters are calculated at BP86/cc-pvTZ, cc-pvTZ-pp level of theory. The corresponding shapes of HOMO–LUMO are presented.

Table 1. Electron Configurations Cr atom and Local Magnetic Moments (LMM in  $\mu_B$ ).

n	Electron Configurations Cr atom		LMM(Cr)			LMM(Cu <sub>n</sub> )		
	$\alpha$ -spin orbital	$\beta$ -spin orbital	4s	4p	3d	4s	4p	3d
9	[core]4s <sup>0.28</sup> 3d <sup>4.62</sup> 4p <sup>0.77</sup> 5d <sup>0.06</sup>	[core]4s <sup>0.21</sup> 3d <sup>1.43</sup> 4p <sup>0.69</sup> 5d <sup>0.04</sup>	0.1	0.0	3.2	-0.4	-0.2	0.2
10	[core]4s <sup>0.26</sup> 3d <sup>4.57</sup> 4p <sup>0.98</sup> 5d <sup>0.06</sup>	[core]4s <sup>0.23</sup> 3d <sup>2.15</sup> 4p <sup>0.91</sup> 5d <sup>0.04</sup>	0.0	0.0	2.4	-0.5	-0.3	0.2
11	[core]4s <sup>0.25</sup> 3d <sup>4.47</sup> 4p <sup>1.19</sup> 5d <sup>0.03</sup>	[core]4s <sup>0.24</sup> 3d <sup>3.15</sup> 4p <sup>1.15</sup> 5d <sup>0.01</sup>	0.0	0.0	1.4	-0.4	-0.3	0.2

The results show that for both alpha and beta spin orbitals of Cr atom the occupancy of 3d-Cr is major. The local magnetic moment of Cr atom gradually decreases from 3.2  $\mu_B$  to 1.4  $\mu_B$  and the total magnetic moment of clusters gradually decreases from 3  $\mu_B$  to 1  $\mu_B$  with increasing the size n from 9 to 11. In this Fig. 2, analyzing the total/partial DOS of n = 9-11 clusters shows that the 3d-Cr orbital contribution in the HOMO peak (at -4.6 eV) of CrCu<sub>9</sub>, CrCu<sub>10</sub>, and CrCu<sub>11</sub> clusters are 56.1 %, 53.2 % and 43.2 %, respectively. For all of the investigated ground-state structures, the total magnetic moment of the clusters is largely localized in the Cr atoms, and their unpaired 3d electrons govern the total magnetic moment of the clusters.

It is surprising that the outermost (3d<sup>5</sup>4s<sup>1</sup>) valence electrons of Cr atom are not fully hybridized and entirely delocalized to form the molecular shell as expected. The molecular diagrams of all three considered clusters indicate a partial hybridization between 3d-Cr and 4s-Cu electrons and interestingly, the molecular shell of 3d-Cr and 4s-Cu electrons and the atomic shell of 3d-Cr electrons both are coexisting. In particular, the Cr atom donates 3, 4, and 5 valence electrons to the molecular shell of Cu<sub>9</sub>, Cu<sub>10</sub>, and Cu<sub>11</sub> to form the electronic configuration 1S<sup>2</sup>1P<sup>6</sup>1D<sup>4</sup>, 1S<sup>2</sup>1P<sup>6</sup>1D<sup>6</sup>, and 1S<sup>2</sup>1P<sup>6</sup>1D<sup>8</sup>, respectively. The remaining 3, 2, and 1 valence electron(s) are localized in the d-orbitals of the Cr atom.

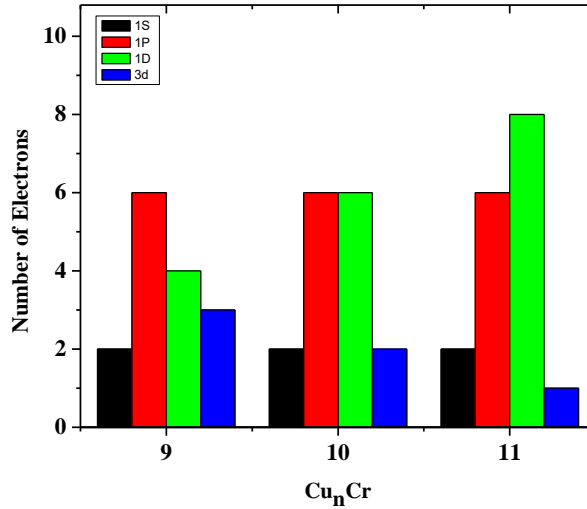


Figure 3. Electronic shell fillings of Cu<sub>n</sub>Cr (n = 9-11). The black, red and green columns in the electron shell filling diagrams represent the occupation of 1S, 1P and 1D shell, respectively. The occupation of the localized 3d Cr orbitals is given by the blue column.

These localized electrons are unpaired causing the magnetic moment of the clusters while the delocalized electrons in the molecular shell are all paired like those in the pure Cu clusters. It

should be mentioned that the pure Cu clusters show a strong odd-even behavior in which the valence electrons prefer to exist in pairs rather than to fill the molecular orbital following the Hund's rule as seen in individual atoms [26]. There is no singly occupied orbital found in the molecular shell since they are less stable (or require more energy) than the  $3d$ -orbital of the Cr atom. This observation is also in a good agreement with the odd-even behavior of pure Cu clusters.

The results from natural orbital analysis are summarized in Fig. 3 where the electronic shell fillings of  $\text{Cu}_n\text{Cr}$  ( $n = 9-11$ ) are presented. It can be seen that when  $n$  goes from 9 to 11, the interior shells (1S and 1P) of the clusters are unaffected. Nevertheless, the number of electrons in the outer shell (1D) is varied as 4, 6, and 8, respectively, in an agreement with the above observation in molecular diagram. At the same time, the number of localized electrons in  $3d$ -Cr orbitals is reduced as 3, 2, and 1, accordingly. The increment of 1D electrons simultaneously comes from  $4s$ -Cu orbitals for added Cu atoms and  $3d$ -Cr localized orbitals.

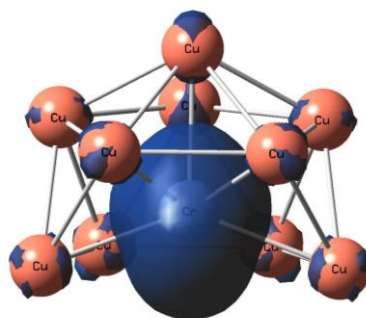


Figure 4. Spin density (blue basin for spin-alpha) of the ground-state  $\text{Cu}_{10}\text{Cr}$  cluster.

As one should be agreed that the  $\text{Cu}_n\text{Cr}$  clusters ( $n = 9-11$ ) possess a certain spin states. In the previous work [23], the results went to the same conclusion that the studied clusters exhibit a magnetic moment but the question about their magnetic origin has not been understood completely yet. By knowing where the unpaired electrons locate, in this report we could pre-empt by our physical intuition that the unpaired electrons are on the  $3d$  orbitals of Cr atom. This picture can be visualized by plotting the spin distribution of the obtained energy minima structures. As demonstrated in Fig. 4, the total spin mainly locates at the dopant position, in line with the above discussion. The exact electronic configurations of  $\text{Cu}_9\text{Cr}$ ,  $\text{Cu}_{10}\text{Cr}$ , and  $\text{Cu}_{11}\text{Cr}$  can be assigned as  $1S^21P^61D^43d_{\text{Cr}}^{3\uparrow}$ ,  $1S^21P^61D^63d_{\text{Cr}}^{2\uparrow}$ , and  $1S^21P^61D^83d_{\text{Cr}}^{1\uparrow}$ , respectively.

#### 4. CONCLUSIONS

The method of density functional theory using the BP86 functional and cc-pvTZ, cc-pvTZ-pp basis set have been employed to optimize geometrical structures following by frequency calculations of the clusters  $\text{Cu}_n\text{Cr}$  ( $n=9-11$ ). Electronic energies, zero point energies, electron configurations and geometries of the clusters have been derived. The  $\text{Cu}_n\text{Cr}$  clusters ( $n = 9-11$ ) possess high spin multiplicities and in this structure there is a superposition of the molecular magnetic shell that form mainly by partial  $3d$ -Cr orbitals and the molecular electronic shell composed by partial  $3d$ -Cr and all  $4s$ -Cu orbitals. We believe that this work will be useful for understanding the physics of magnetic impurities in noble metal clusters and could lead to a rational design of outperforming superatoms with a desired magnetic feature.

**Acknowledgements.** This work is supported by Institute of Materials Science, Vietnam Academy of Science and Technology.

## REFERENCES

1. Claes P., Ngan V. T., Haertelt M., Lyon J. T., Fielicke A., Nguyen M. T., Lievens P., and Janssens E. - The structures of neutral transition metal doped silicon clusters,  $\text{Si}_n\text{X}$  ( $n = 6-9$ ;  $\text{X} = \text{V}, \text{Mn}$ ), *J. Chem. Phys.* **138** (2013) 194301.
2. Tung N. T., Janssens E., and Lievens P. - Dopant dependent stability of  $\text{Co}_n\text{TM}^+$  ( $\text{TM} = \text{Ti}, \text{V}, \text{Cr}, \text{and Mn}$ ) clusters, *Appl. Phys. B* **114** (2014) 497-502.
3. Tung N. T., Tam N. M., Nguyen M. T., Lievens P., and Janssens E. - Influence of Cr doping on the stability and structure of small cobalt oxide clusters, *J. Chem. Phys.* **141** (2014) 044311.
4. Ngan V. T., Janssens E., Claes P., Lyon J. T., Fielicke A., Nguyen M. T., and Lievens P. - High magnetic moments in manganese-doped silicon clusters, *Chem. Eur. J.* **18** (2012) 15788-15793.
5. Die D., Kuang X. Y., Gua J. J., Zheng B. X. - Density functional theory study of  $\text{Au}_n\text{Mn}(n=1-8)$  clusters, *J. Phys. Chem. Solids* **71** (2010) 770-775.
6. Wang H. Q., Kuang X. Y., Li H. F. - Density functional study of structural and electronic properties of bimetallic copper-gold clusters: comparison with pure and doped gold clusters, *Phys. Chem. Chem. Phys.* **12** (2010) 5156-5165.
7. Li G., Wang K., Wang Q., Zhao Y., Du J., He J. - Formation of icosahedral and hcp structures in bimetallic Co-Cu clusters during the freezing processes, *Mater. Lett.* **88** (2012) 126-128.
8. Ma W., Chen F. - Optical and electronic properties of Cu doped Ag clusters, *J. Alloys Compd.* **541** (2012) 79-83.
9. Cheng X. H., Ding D. J., Yu Y. G., Jin M. X. - Geometrical Structures and Electronic Properties of Copper-Doped Aluminum Clusters, *J. Chem. Phys.* **25** (2012) 169-176.
10. Wang L. M., Pal R., Huang W., Zeng X. C., Wang L. S. - Observation of earlier two-to-three dimensional structural transition in gold cluster anions by isoelectronic substitution:  $\text{MAu}_n^-$  ( $n = 8-11$ ;  $M = \text{Ag}, \text{Cu}$ ), *J. Chem. Phys.* **132** (2010) 114306.
11. Cox D. M., Zakin M. R., and Kaldor A. - Size selective chemical and physical properties of clusters, (1987) US TUA2.
12. Zhou Y. H., Zeng Z., Ju X. - The structural and electronic properties of  $\text{Cu}_m\text{Ag}_n$  ( $m + n = 6$ ) clusters, *Microelectron. J.* **40** (2009) 832-834.
13. Wang Ling., Die Dong., Wang Shi-Jian., Zhao Zheng-Quan. - Geometrical, electronic, and magnetic properties of  $\text{Cu}_n\text{Fe}$  ( $n = 1-12$ ) clusters: A density functional study, *J. Chem. Phys. Solids* **76** (2015) 10-16.
14. Bagayoko D., Blaha P., Callaway J. - Electronic structure of chromium and manganese impurities in copper, *Phys. Rev.* **34** (1986) 3572-3576.
15. Florez E., Mondragon F., Illas F. - Theoretical study of the structure and reactivity descriptors of  $\text{Cu}_n\text{M}$  ( $M = \text{Ni}, \text{Pd}, \text{Pt}$ ;  $n = 1-4$ ) bimetallic nanoparticles supported on  $\text{MgO}(001)$ , *Surf. Sci.* **606** (2012) 1010-1018.

16. Jiang Z. Y., Lee K. H., Li S. T., Chu S. Y. - Structures and charge distributions of cationic and neutral  $\text{Cu}_{n-1}\text{Ag}$  clusters ( $n = 2-8$ ), *Phys. Rev. B* **73** (2006) 235423.
17. Bandyopadhyay D. - Architectures, electronic structures, and stabilities of Cu-doped  $\text{Ge}_n$  clusters: density functional modeling, *J. Mol. Model.* **18** (2012) 3887–3902.
18. Wang J., and Ju-Guang Han - A computational investigation of copper-doped germanium and germanium clusters by the density-functional theory, *J Chem Phys.* **123** (2005) 244303.
19. Ngan V. T., Gruene P., Claes P., Janssens E., Fielicke A., Nguyen M. T., and Lievens P. - Disparate Effects of Cu and V on Structures of Exohedral Transition Metal-Doped Silicon Clusters: A Combined Far-Infrared Spectroscopic and Computational Study *J. Am. Chem. Soc.* **132** (2010) 15589-15602.
20. Mejía-López J., García G., and Romero A. H. - Physical and chemical characterization of  $\text{Pt}_{12-n}\text{Cu}_n$  clusters via *ab initio* calculations, *J. Chem. Phys.* **131** (2009) 044701.
21. Veldeman N., Holtzl T., Neukermans S., Veszpremi T., Nguyen M. T., Lievens P. - Experimental observation and computational identification of  $\text{Sc}@\text{Cu}^+_{16}$ , a stable dopant-encapsulated copper cage, *Phys. Rev. A* **76** (2007) 011201.
22. Sun Q., Gong X. G., Zheng Q. Q., Wang G. H. - First-principles study of the magnetic properties of 4d impurities in  $\text{Cu}_n$  clusters, *Phys. Lett. A* **209** (1995) 249-253.
23. Pham H. T, Cuong N. T., Tam N. M., and Tung N. T. - A systematic investigation on  $\text{CrCu}_n$  clusters with  $n = 9-16$ : Noble gas and tunable magnetic property, *J. Phys. Chem. A* **120** (2016) 7335-7343.
24. Frisch M.J, Schlegel H. B., Scuseria G. E., Robb M. A., Cheeseman J. R, et al., Gaussian 09, Revision A.02, Gaussian, Inc., Wallingford CT, (2009).
25. Hohenberg P., and Kohn W. - Inhomogeneous Electron Gas, *Phys. Rev. B*, **136** (1964) 864.
26. Li C. G., Shen Z. G., Hu Y. F., Tang Y. N., Chen W. G., and Ren B. Z. - Insights into the structures and electronic properties of  $\text{Cu}_{n+1}^{\mu}$  and  $\text{Cu}_n\text{S}^{\mu}$  ( $n = 1-12$ ;  $\mu = 0, \pm 1$ ) clusters, *Sci. Rep.* **7** (2017) 1345.